Stat. Phys. IV: Summary slides on the lecture 8

Spring 2025

The Jarzynski equation[1]

Work on a system connected to a reservoir at T, between states with difference of free energy ΔF (Helmholtz free energy). In general, we have $W \geq \Delta F$.
Jarzynski equality relates Helmholtz free energy differences between two states and the irreversible work along an ensemble of trajectories joining the same states. Jarzinski equality is valid, regardless of how fast (out of equilibrium) is the process between the two states. It just required two initial and final states to be in the thermal equilibrium.

Jarzynski equality

$$\langle \exp(-\beta W) \rangle = \int \exp(-\beta W)\, P(W, t_s) dW = \exp(-\beta \Delta F), \quad \beta = 1/k_B T$$

[1] C. Jarsynski, "Nonequilibrium Equality for Free Energy Differences" PRL 1997 and G. E. Crooks, "Entropy production fluctuation theorem and the nonequilibrium work relation for free energy differences" PRE 1999.

The Crooks theorem[2]

The Crooks theorem says if the dynamics of the system satisfies microscopic reversibility, then the forward time trajectory is exponentially more likely than the reverse.

Crooks theorem

$$\frac{P_f(W)}{P_b(-W)} = \exp\left(\frac{W - \Delta F}{k_B T}\right)$$

with the probability distribution of the work done during the forward and backward processes.

[2] C. Jarsynski, "Nonequilibrium Equality for Free Energy Differences" PRL 1997 and G. E. Crooks, "Entropy production fluctuation theorem and the nonequilibrium work relation for free energy differences" PRE 1999.

Verification of Crooks Fluctuation Theorem[3]

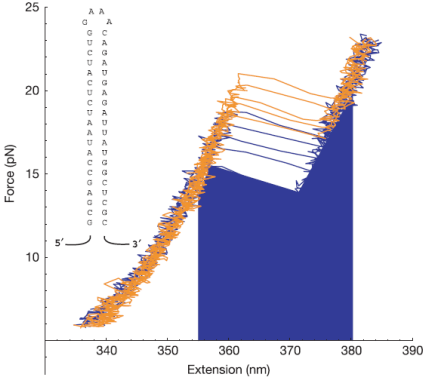

Figure 1 | Force-extension curves. The stochasticity of the unfolding and refolding process is characterized by a distribution of unfolding or refolding work trajectories. Five unfolding (orange) and refolding (blue) force–extension curves for the RNA hairpin are shown (loading rate of 7.5 pN s^{-1}). The blue area under the curve represents the work returned to the machine as the molecule switches from the unfolded to the folded state. The RNA sequence is shown as an inset.

[3] D. Collin *et al.*, Nature **437** 231-234 (2005)

Verification of Crooks Fluctuation Theorem[4]

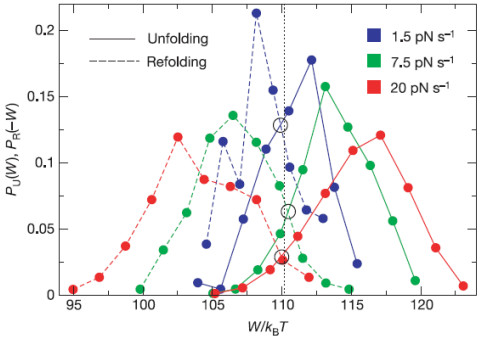

Figure 2 | Test of the CFT using an RNA hairpin. Work distributions for RNA unfolding (continuous lines) and refolding (dashed lines). We plot negative work, $P_R(-W)$, for refolding. Statistics: 130 pulls and three molecules ($r = 1.5\,\mathrm{pN\,s^{-1}}$), 380 pulls and four molecules ($r = 7.5\,\mathrm{pN\,s^{-1}}$), 700 pulls and three molecules ($r = 20.0\,\mathrm{pN\,s^{-1}}$), for a total of ten separate experiments. Good reproducibility was obtained among molecules (see Supplementary Fig. S2). Work values were binned into about ten equally spaced intervals. Unfolding and refolding distributions at different speeds show a common crossing around $\Delta G = 110.3\,k_BT$.

[4] D. Collin *et al.*, Nature **437** 231-234 (2005)

Verification of Crooks Fluctuation Theorem[5]

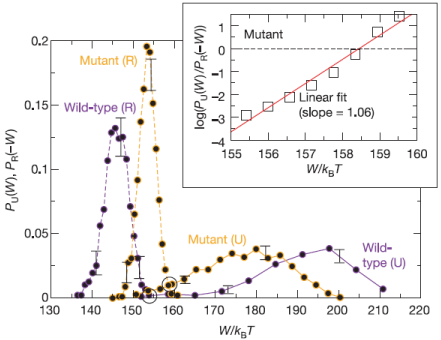

Figure 3 | Free-energy recovery and test of the CFT for non-gaussian work distributions. Experiments were carried out on the wild-type and mutant S15 three-helix junction without Mg^{2+}. Unfolding (continuous lines) and refolding (dashed lines) work distributions. Statistics: 900 pulls and two molecules (wild type, purple); 1,200 pulls and five molecules (mutant type, orange). Crossings between distributions are indicated by black circles. Work histograms were found to be reproducible among different molecules (error bars indicating the range of variability). Inset, test of the CFT for the mutant. Data have been linearly interpolated between contiguous bins of the unfolding and refolding work distributions.

[5] D. Collin *et al.*, Nature **437** 231-234 (2005)

Experimental test of Jarzynski's equality[6]

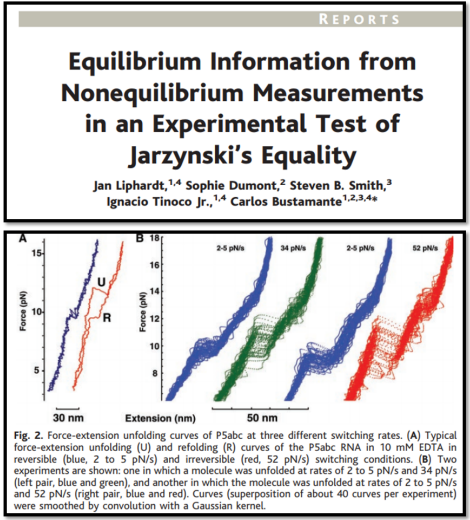

REPORTS

Equilibrium Information from Nonequilibrium Measurements in an Experimental Test of Jarzynski's Equality

Jan Liphardt,[1,4] Sophie Dumont,[2] Steven B. Smith,[3] Ignacio Tinoco Jr.,[1,4] Carlos Bustamante[1,2,3,4]*

Fig. 2. Force-extension unfolding curves of P5abc at three different switching rates. (**A**) Typical force-extension unfolding (U) and refolding (R) curves of the P5abc RNA in 10 mM EDTA in reversible (blue, 2 to 5 pN/s) and irreversible (red, 52 pN/s) switching conditions. (**B**) Two experiments are shown: one in which a molecule was unfolded at rates of 2 to 5 pN/s and 34 pN/s (left pair, blue and green), and another in which the molecule was unfolded at rates of 2 to 5 pN/s and 52 pN/s (right pair, blue and red). Curves (superposition of about 40 curves per experiment) were smoothed by convolution with a Gaussian kernel.

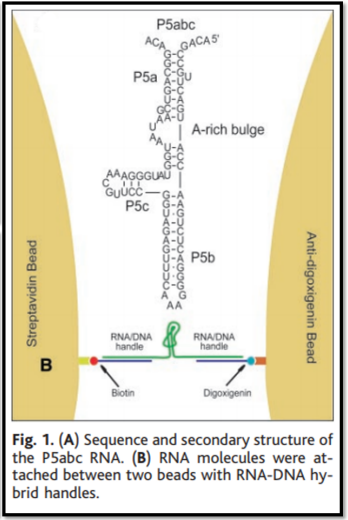

Fig. 1. (**A**) Sequence and secondary structure of the P5abc RNA. (**B**) RNA molecules were attached between two beads with RNA-DNA hybrid handles.

[6] J. Liphardt *et al.*, Science **296** 1832-1835 (2002)

Jarzynski equality

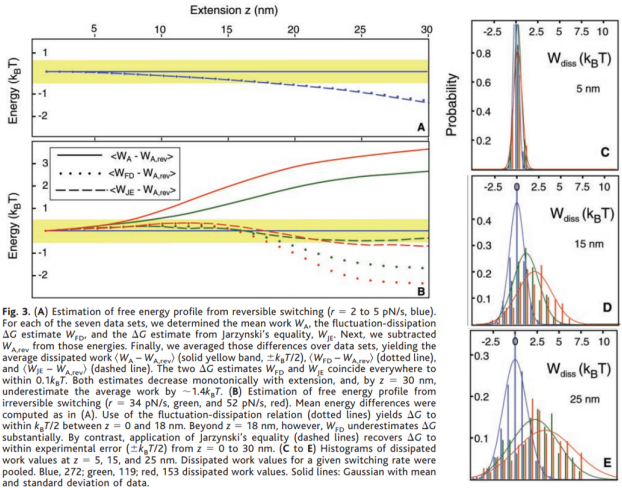

Fig. 3. (**A**) Estimation of free energy profile from reversible switching (r = 2 to 5 pN/s, blue). For each of the seven data sets, we determined the mean work W_A, the fluctuation-dissipation ΔG estimate W_{FD}, and the ΔG estimate from Jarzynski's equality, W_{JE}. Next, we subtracted $W_{A,rev}$ from those energies. Finally, we averaged those differences over data sets, yielding the average dissipated work $\langle W_A - W_{A,rev}\rangle$ (solid yellow band, $\pm k_BT/2$), $\langle W_{FD} - W_{A,rev}\rangle$ (dotted line), and $\langle W_{JE} - W_{A,rev}\rangle$ (dashed line). The two ΔG estimates W_{FD} and W_{JE} coincide everywhere to within $0.1k_BT$. Both estimates decrease monotonically with extension, and, by z = 30 nm, underestimate the average work by $\sim 1.4k_BT$. (**B**) Estimation of free energy profile from irreversible switching (r = 34 pN/s, green, and 52 pN/s, red). Mean energy differences were computed as in (**A**). Use of the fluctuation-dissipation relation (dotted lines) yields ΔG to within $k_BT/2$ between z = 0 and 18 nm. Beyond z = 18 nm, however, W_{FD} underestimates ΔG substantially. By contrast, application of Jarzynski's equality (dashed lines) recovers ΔG to within experimental error ($\pm k_BT/2$) from z = 0 to 30 nm. (**C** to **E**) Histograms of dissipated work values at z = 5, 15, and 25 nm. Dissipated work values for a given switching rate were pooled. Blue, 272; green, 119; red, 153 dissipated work values. Solid lines: Gaussian with mean and standard deviation of data.

Spectral line example

- An observed data set D, for spectral line shape: at frequencies ν_i, signal strength d_i is measured.
- A model for spectral line shape with two parameters T and ν:

$$T \cdot \exp\left(\frac{-(\nu_i - \nu)^2}{\sigma^2}\right) = T \cdot f_i$$

- Prior information:
  Uniform distribution for ν ($P(\nu|I)$) and Jeffrey's prior for T ($P(T|I)$).
- likelihood function: $P(D|Y, I) = \frac{1}{\sqrt{(2\pi\sigma^2)^N}} \exp\{-\frac{\sum_i (d_i - T f_i)^2}{2\sigma^2}\}$
- Metropolis rate:

$$r = \frac{P(Y|D, I)}{P(X_t|D, I)} = \frac{P(T', \nu'|I) P(D|T', \nu', I)}{P(T_t, \nu_t|I) P(D|T_t, \nu_t, I)}$$

Spectral line example

Spectral line data consisting of 64 frequency channels obtained with a radio astronomy spectrometer

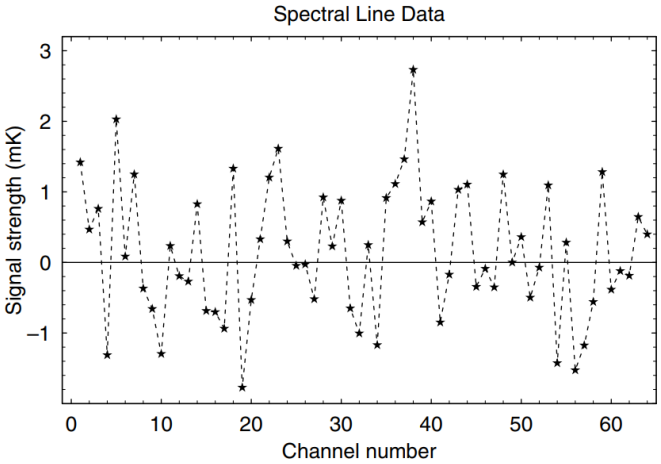

Bayesian Inference [7]

Updating a statistical model (H_i) using an observed data set (D) and a prior information (I). According to Bayes theorem:

Posterior probability distribution

$$P(H_i|D,I) = \frac{P(H_i|I)P(D|H_i,I)}{P(D|I)}$$

- $P(H_i|D,I)$: The probability after observation of D (posterior).
- $P(H_i|I)$: The probability before observation of D (prior).
- $P(D|H_i,I)$: The probability of observing D given the model H_i (likelihood).
- $P(D|I)$: The probability of observing D given the prior information (global likelihood).

[7] Chapters 3 *Bayesian Logical Data Analysis for the Physical Sciences* P. C. Gregory

Markov Chain Monte Carlo (MCMC)[8]

For a model with set of parameters $\{X\}$ generate a random walk in the parameter (estimation) space such that the probability of being in the region is proportional to the posterior PDF.

Metropolis-Hastings algorithm

1. Initialize model parameters X_0.
2. obtain a random sample for model parameters (e.g with Normal probability distributions).
3. Calculate Metropolis ratio: $r = \frac{P(Y|D,I)}{P(X_t|D,I)}$ with X_t being model parameters at time step t. Acceptance probability (transition rate): $W_{X_t,Y} = min(1, r)$
4. If $r < 1$, obtain a uniformly distributed random number between 0 and 1 called u and:

$$\textit{if } u \leq r : X_{t+1} = Y, \textit{otherwise: } X_{t+1} = X_t$$

5. return to step 2.

[8] Chapters 12 *Bayesian Logical Data Analysis for the Physical Sciences* P. C. Gregory

Quantization of an electrical circuit

We consider the classical energy of an LC circuit where Q is the charge on the capacitor and ϕ the magnetic flux.

Quantization of the Hamiltonian

$$H = \frac{Q^2}{2C} + \frac{\phi^2}{2L} \to \hat{H} = \frac{\hat{Q}^2}{2C} + \frac{\hat{\phi}^2}{2L} \qquad \text{with} \quad [\hat{\phi}, \hat{Q}] = i\hbar$$

Charge and flux can be expressed with the creation and annihilation operators as one can write

$$\hat{\phi} = \phi_{zpf}(\hat{a} + \hat{a}^\dagger) \qquad \phi_{zpf} = \sqrt{\frac{\hbar}{2}\sqrt{\frac{L}{C}}}$$

$$\hat{Q} = Q_{zpf}\frac{(\hat{a} - \hat{a}^\dagger)}{i} \qquad Q_{zpf} = \sqrt{\frac{\hbar}{2}\sqrt{\frac{C}{L}}}$$

Inserting this and using the commutation relation $[\hat{a}, \hat{a}^\dagger] = 1$ yield:

$$\hat{H} = \frac{\hbar}{2\sqrt{LC}}\left(\hat{a}^\dagger\hat{a} + \hat{a}\hat{a}^\dagger\right) = \hbar\omega\left(\hat{a}^\dagger\hat{a} + \frac{1}{2}\right)$$

Quantization of an electrical circuit[9]

Even the ground state $|0\rangle$ has fluctuations called

Zero-point fluctuations

$$\phi_{zpf}^2 = (\Delta\phi)_{|0\rangle}^2 = \langle 0|\hat{\phi}^2|0\rangle - \langle 0|\hat{\phi}|0\rangle^2 = \frac{\hbar}{2}\sqrt{\frac{L}{C}}$$
$$Q_{zpf}^2 = (\Delta Q)_{|0\rangle}^2 = \langle 0|\hat{Q}^2|0\rangle - \langle 0|\hat{Q}|0\rangle^2 = \frac{\hbar}{2}\sqrt{\frac{C}{L}}$$

They respect the Heisenberg uncertainty principle: $\left[(\Delta Q)_{|0\rangle}(\Delta\phi)_{|0\rangle} = \hbar/2\right] \geq \hbar/2$.

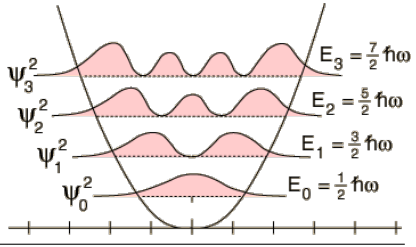

Wavefunction representation of the first eigenstates of a harmonic oscillator.

[9] See e.g. Quantum Optics 1 by A. Aspect and M. Brune, week 1, on Coursera.

Coherent states

We consider a quantum harmonic oscillator of resonance frequency ω.
Properties of Fock states $|n\rangle$:

- $\hat{a}\,|n\rangle = \sqrt{n}\,|n-1\rangle$ and $\hat{a}^\dagger\,|n\rangle = \sqrt{n+1}\,|n+1\rangle$
- time evolution: $|n(t)\rangle = e^{-i\omega n t}\,|n(0)\rangle$

Definition of a coherent state

$$|\alpha\rangle \equiv e^{-|\alpha|^2/2} \sum_{n=0}^{\infty} \alpha^n \frac{|n\rangle}{\sqrt{n!}}$$

Properties of coherent states $|\alpha\rangle$:

- $\hat{a}\,|\alpha\rangle = \alpha\,|\alpha\rangle$
- Poisson statistics: $\langle\hat{n}\rangle = \langle\alpha|\hat{a}^\dagger\hat{a}|\alpha\rangle = |\alpha|^2$ and $\langle\hat{n}^2\rangle - \langle\hat{n}\rangle^2 = |\alpha|^2$
- time evolution: $|\alpha(t)\rangle = |e^{-i\omega t}\alpha(0)\rangle$

Coherent states and P-function[10]

Bargmann states: unnormalized coherent states $||\alpha\rangle = \sum_{n=0}^{\infty} \alpha^n \frac{|n\rangle}{\sqrt{n!}}$ with the property $\hat{a}^\dagger ||\alpha\rangle = \partial_\alpha ||\alpha\rangle$.

The set of coherent states is overcomplete: $\hat{I} = \frac{1}{\pi} \int d^2\alpha |\alpha\rangle\langle\alpha|$ ($\hat{I}$ is the identity operator).

Density matrix decomposition in terms of coherent states

$$\hat{\rho} = \int P(\alpha)|\alpha\rangle\langle\alpha| d^2\alpha,$$

where $P(\alpha) = 1/\pi \int \langle -\beta|\hat{\rho}|\beta\rangle \exp(|\beta|^2 - \beta\alpha^* + \beta^*\alpha + |\alpha|^2) d^2\beta$ is the Glauber-Sudarshan phase space function.

[10] "Stochastic Methods", C. Gardiner, Chapter 10.

Next week's presentation

PRL 99, 093902 (2007) PHYSICAL REVIEW LETTERS week ending 31 AUGUST 2007

Quantum Theory of Cavity-Assisted Sideband Cooling of Mechanical Motion

Florian Marquardt,[1] Joe P. Chen,[2,4] A. A. Clerk,[3] and S. M. Girvin[2]

[1]*Department of Physics, Arnold-Sommerfeld-Center for Theoretical Physics, and Center for NanoScience, Ludwig-Maximilians-Universität München, Theresienstrasse 37, 80333 Munich, Germany*
[2]*Department of Physics, Yale University, P.O. Box 208120, New Haven, Connecticut 06520-8120, USA*
[3]*Department of Physics, McGill University, 3600 rue University, Montreal, QC Canada H3A 2T8*
[4]*Department of Physics, Cornell University, 109 Clark Hall, Ithaca, New York 14853-2501, USA*

(Received 22 January 2007; published 28 August 2007)

We present a quantum-mechanical theory of the cooling of a cantilever coupled via radiation pressure to an illuminated optical cavity. Applying the quantum noise approach to the fluctuations of the radiation pressure force, we derive the optomechanical cooling rate and the minimum achievable phonon number. We find that reaching the quantum limit of arbitrarily small phonon numbers requires going into the good-cavity (resolved phonon sideband) regime where the cavity linewidth is much smaller than the mechanical frequency and the corresponding cavity detuning. This is in contrast to the common assumption that the mechanical frequency and the cavity detuning should be comparable to the cavity damping.

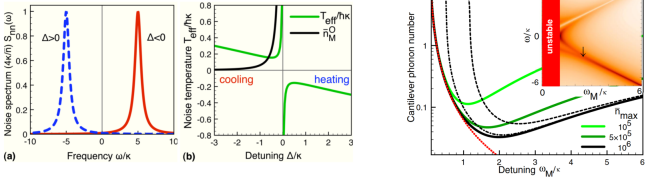

Questions for next week's paper presentation

- Introduce the optomechanical interaction and its Hamiltonian
- What is the power spectral density (PSD) of the radiation pressure and how it related to the cooling/heating of the mechanical mode
- Explain how by choosing the correct cavity detuning, the interaction can result in cooling of the mechanical mode. What is the phonon occupation of the mechanical mode at the steady state?
- Present the complete description of the problem using the quantum Langevin equations